

CHAPTER 5

DISCUSSION AND CONCLUSIONS

The main aims of this project were stated at the end of Chapter 1 (see page 19). In this final Chapter 5, the extent to which these aims have been achieved will become apparent as the results are discussed and the appropriate conclusions drawn.

5.1 Physical Characterisation of 'Maxon' and 'PDS II'

Solubility testing of 'Maxon' showed that the polymer does not dissolve in common organic solvents, either hot or cold. 'PDS II', on the other hand, was soluble in hot chloroform at 60-65 °C. However, following tests on a wide range of different solvents, the most effective was found to be dimethylsulfoxide (DMSO) at 130 °C for 'Maxon' and 120 °C for 'PDS II'. Absolute ethanol and methanol were found to be suitable non-solvents, the polymers precipitating from hot DMSO solution in the form of finely-divided powders, white-coloured for 'PDS II' and cream-coloured for 'Maxon'.

Thermal analysis also revealed some interesting features. Considering that it is an aliphatic copolyester, 'Maxon' has an unusually high melting range, T_m , of 192-215 °C. In marked contrast, 'PDS II' has a much lower melting range, T_m , of 93-112 °C, typical of aliphatic polyesters.

Polymer melting is a pseudo-equilibrium process which can be discussed in thermodynamic terms [26] via the equation:

$$\Delta G_m = \Delta H_m - T_m \Delta S_m \quad \dots(5.1)$$

where ΔG_m , ΔH_m and ΔS_m are the changes in Gibbs' free energy, enthalpy and entropy of melting respectively at temperature T_m . Melting takes place when the free energy of the process is zero, i.e.,

$$\Delta G_m = \Delta H_m - T_m \Delta S_m = 0 \quad \dots(5.2)$$

Hence,
$$T_m = \Delta H_m / \Delta S_m \quad \dots(5.3)$$

Thus, a polymer's melting point (or range), T_m , is determined by its $\Delta H_m / \Delta S_m$ ratio.

From the planar zig-zag molecular arrangements of 'Maxon' and 'PDS II' in the crystal, as shown in Figs. 5.1 and 5.2, two types of intermolecular interactions can be expected:

(a) dipole-dipole interactions (as in $\overset{\delta^-}{\text{C}}=\text{O} \cdots \text{C}=\overset{\delta^+}{\text{O}}$);

and (b) methylene interactions.

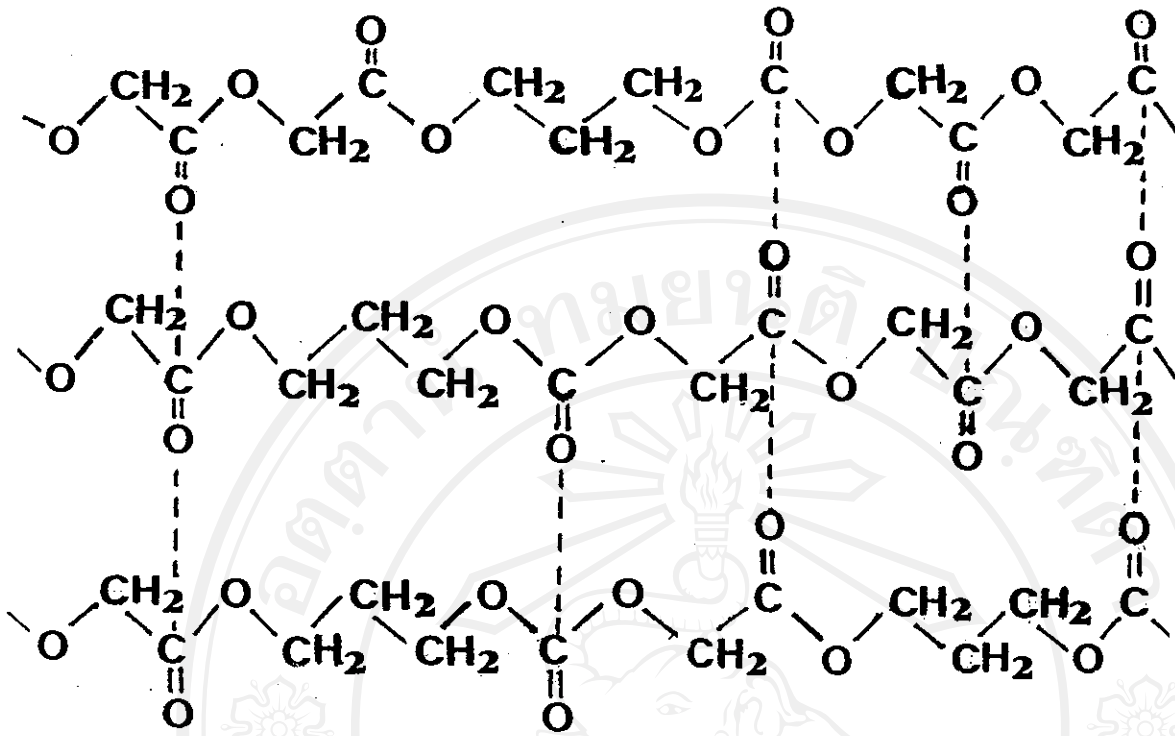


Fig. 5.1: Planar zig-zag molecular arrangement in the 'Maxon' crystal.

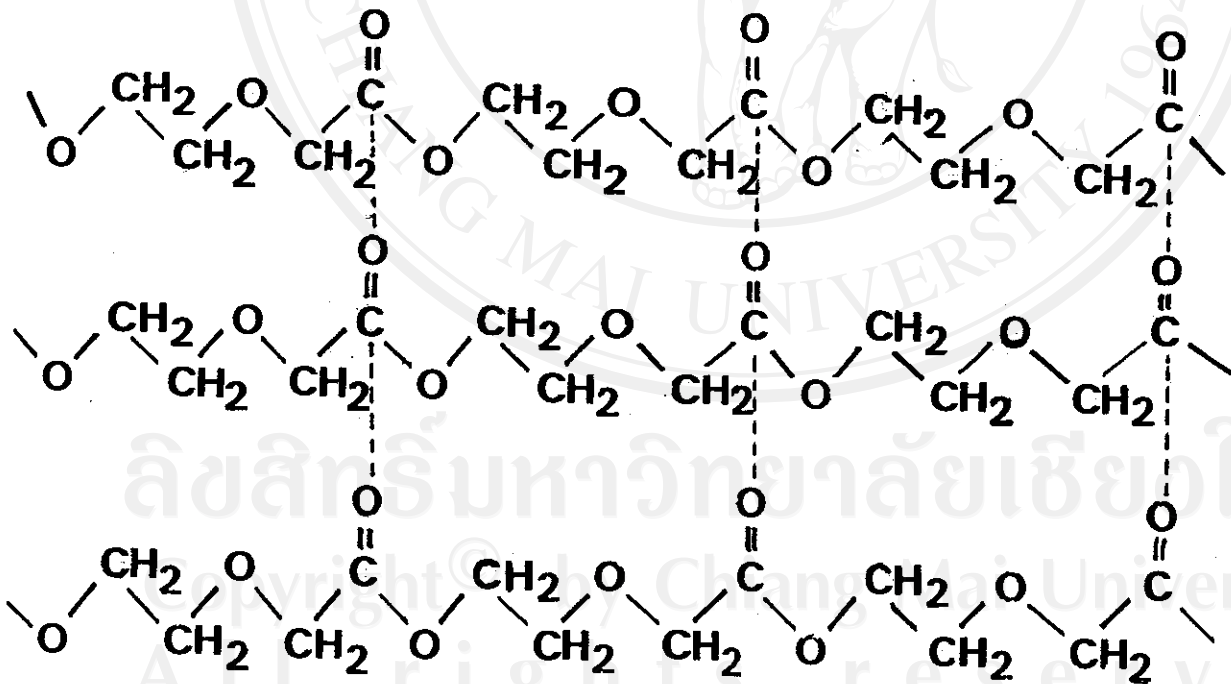


Fig. 5.2: Planar zig-zag molecular arrangement in the 'PDS II' crystal.

As seen in Figs. 5.1 and 5.2, 'Maxon' is richer in ester groups per unit length of the polymer chain than 'PDS II', leading to a higher concentration of dipole-dipole interactions. It is these dipolar forces, rather than the relatively weak methylene interactions, which give rise to a higher than normal ΔH_m in 'Maxon' and, therefore, higher T_m . Another contributing factor is the lowering of ΔS_m due to the partial reforming of the dipole-dipole interactions in the melt state. This explains 'Maxon's' high crystallinity (usually about 40-50%), high melting range, and difficult solubility. 'PDS II', on the other hand, has a longer repeat unit which also incorporates a flexible ether (C-O-C) linkage. These structural differences combine to lower ΔH_m , the energy barrier to chain rotation in the crystal, and increase ΔS_m due to fewer ester groups and a greater degree of chain flexibility in the melt. Thus, 'PDS II' has a lower T_m than 'Maxon'.

5.2 Interpretation of the 'In Vitro' Biodegradation Profiles of 'Maxon' and 'PDS II'

The property changes in 'Maxon' and 'PDS II' during their 'in vitro' biodegradations are shown in the form of composite graphs in Figs. 5.3 and 5.4 respectively. On the basis of these results, an insight into the biodegradation mechanism is now discussed. For the purposes of this discussion, two distinct stages can be identified: (1) before, and (2) after the onset of weight loss.

Stage 1: Before Initial Weight Loss

As seen in Figs. 5.3 and 5.4, the suture weights only started to decrease significantly after about week 9 for 'Maxon' and week 11 for 'PDS II'. However, during these time periods, both sutures underwent immediate and complete reductions in their knot pull strengths to immeasurably low values. These reductions were accompanied by somewhat slower but obviously related reductions in intrinsic viscosity.

These results indicate that the hydrolytic degradations of both 'Maxon' and 'PDS II' commence very early on, during week 1, leading to immediate decreases in polymer molecular weight. Simple hydrolysis of aliphatic polyesters is believed to be a random chain scission process resulting in a rapid reduction to relatively low molecular weight fragments, as illustrated in Fig. 5.5 for 'PDS II'. This hydrolysis reaction can be base - catalysed in an aqueous medium of $\text{pH} > 7$ (as in this case where the $\text{pH} = 7.4$) or acid - catalysed in the event that the new COOH end-groups formed caused the pH of the medium to drop below 7.

As would be expected, the knot pull breaking force profiles in Figs. 5.3 and 5.4 are closely paralleled by those of the intrinsic viscosity. Thus, the results obtained comply with the known interdependence of mechanical strength and molecular weight. The implications of these results for the sutures' performance in actual surgery are obvious. If the suture is to fulfil its primary function as a "temporary scaffold", it needs to retain sufficient tensile strength for a sufficient period of time during which collagen synthesis takes place. The collagen then takes over the role of

keeping the wound surfaces in apposition as the wound continues to heal. The time period for the suture to support initial wound healing is generally considered to be between 1 - 3 weeks, depending on various factors such as the area of the incision and the health of the patient.

From Figs. 5.3 and 5.4, despite the marked changes in intrinsic viscosity and knot pull breaking force, there is very little (< 5 %) accompanying weight loss in either suture during the first 8 weeks. This must be because the low molecular weight chain fragments of 'Maxon' and 'PDS II', formed as a result of hydrolysis, are still unable to diffuse out of the degrading matrix. This is presumably due to the fact that they are still too large compared with the small water molecules which can easily diffuse in.

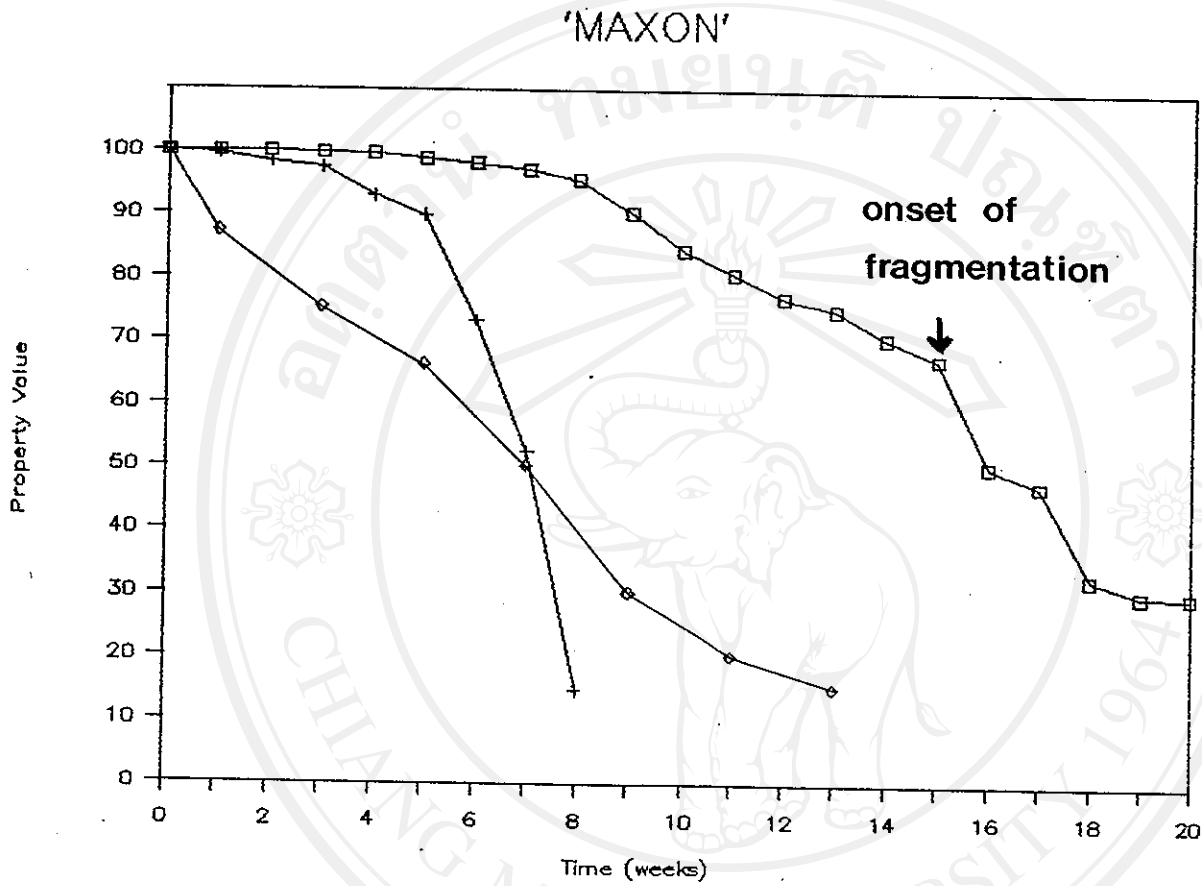


Fig. 5.3: Property changes during the 'in vitro' biodegradation of 'Maxon' immersed in phosphate buffer (37°C, pH 7.40).

- % weight remaining
- + % knot pull force retention
- ◇ % intrinsic viscosity retention

'PDS II'

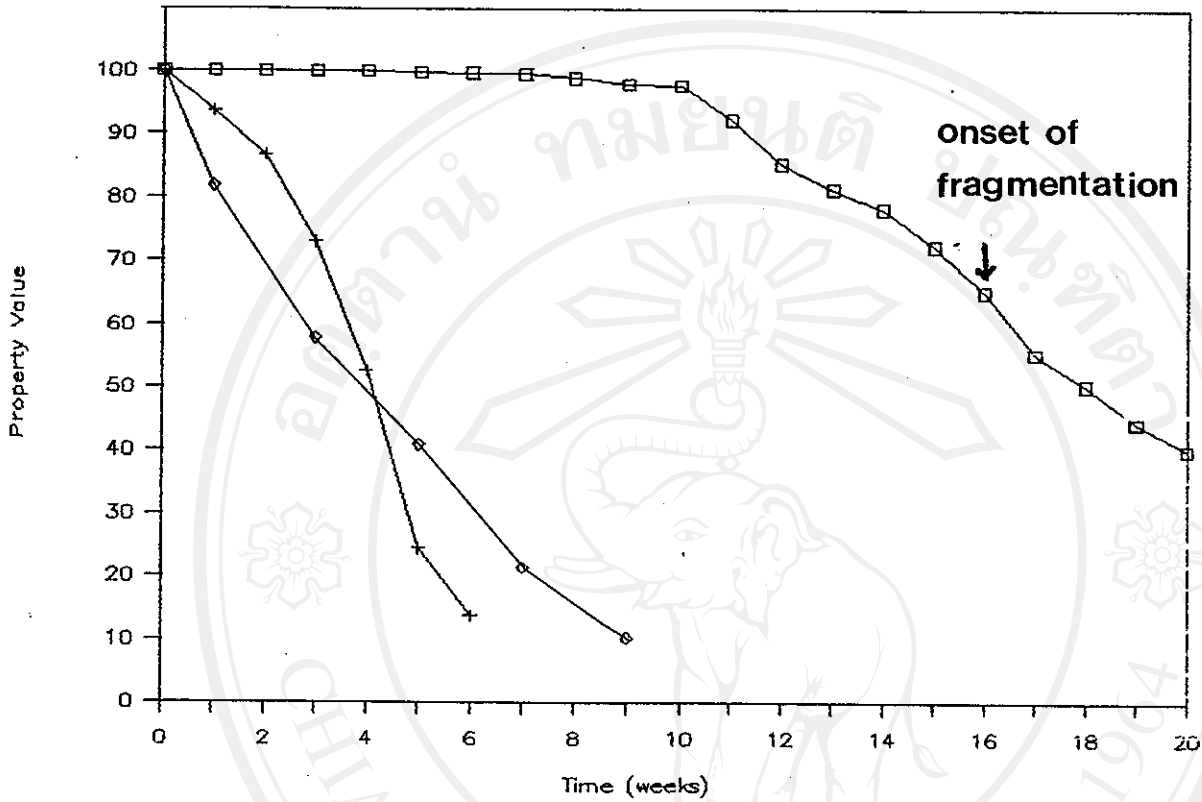


Fig. 5.4 : Property changes during the 'in vitro' biodegradation of 'PDS II' immersed in phosphate buffer (37°C, pH 7.40).

□ % weight remaining

+ % knot pull force retention

◇ % intrinsic viscosity retention

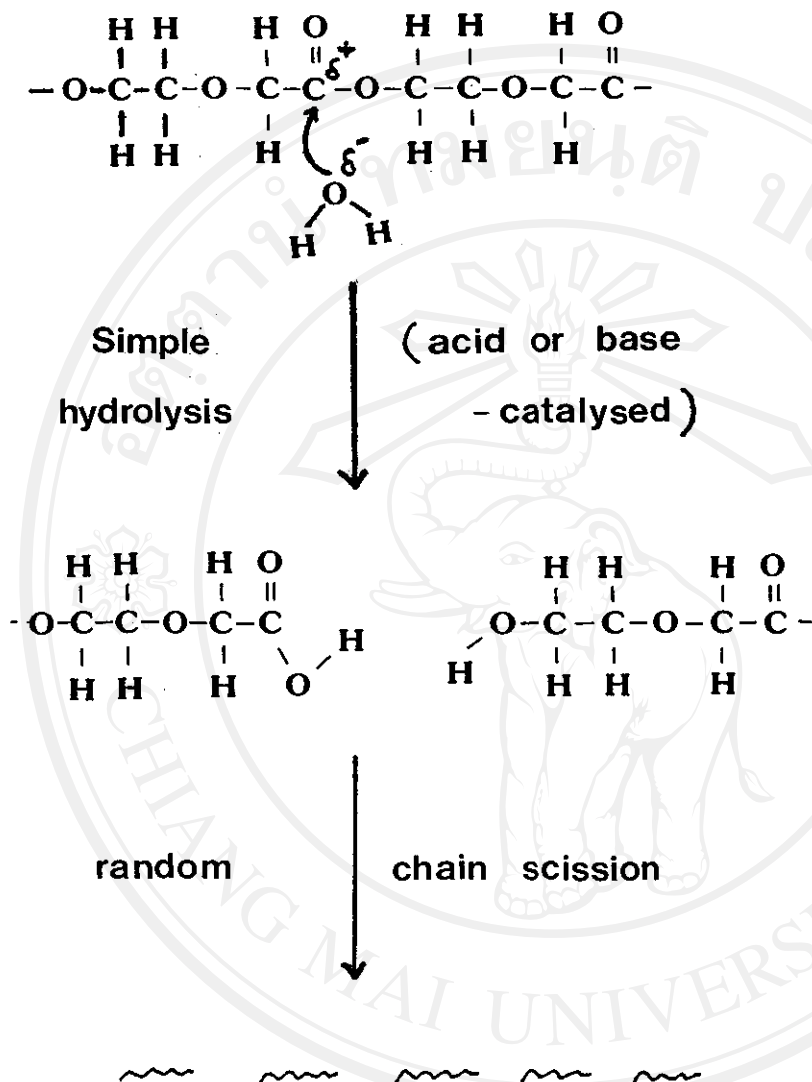


Fig. 5.5 : Simple ester hydrolysis in 'PDS II' leading to random chain scission and rapid molecular weight reduction.

STAGE 2: After Initial Weight Loss

The sudden onset of significant weight loss marks the transition between Stages 1 and 2. As seen in Figs. 5.3 and 5.4, this transition occurs around the end of week 9 for 'Maxon' and week 11 for 'PDS II'. Weight loss represents the diffusion out of the polymer matrix of low molecular weight hydrolysis products. As this matrix erosion proceeds, the porosity of the matrix would be expected to increase, thus allowing further diffusion in of water and diffusion out of degradation products to continue more effectively. However, the fact that the weight loss profiles for both 'Maxon' and 'PDS II' are approximately linear with time suggests that their absorptions are kinetically zero-order. This, in turn, suggests that the rate of weight loss is limited by some controlling factor(s) such as the diffusion of hydrolysis products through the matrix and/or the surface area of the degrading suture in contact with the immersion medium. These and other physico-chemical processes will be discussed in more detail in the next section.

From references [5, 11], it was reported that 'PDS' absorbs 'in vivo' in approximately 160-180 days (23-26 weeks) and loses its tensile strength in approximately 56 - 60 days (8 - 9 weeks). The results of this work would seem to agree quite well with these findings.

5.3 A Mechanistic View of Suture Absorption

On the basis of the foregoing discussion, together with relevant literature information, an overall impression of the mechanism of suture absorption can be formulated. This impression is represented diagrammatically in Fig. 5.6 in which the various physical, chemical and biological processes involved are given.

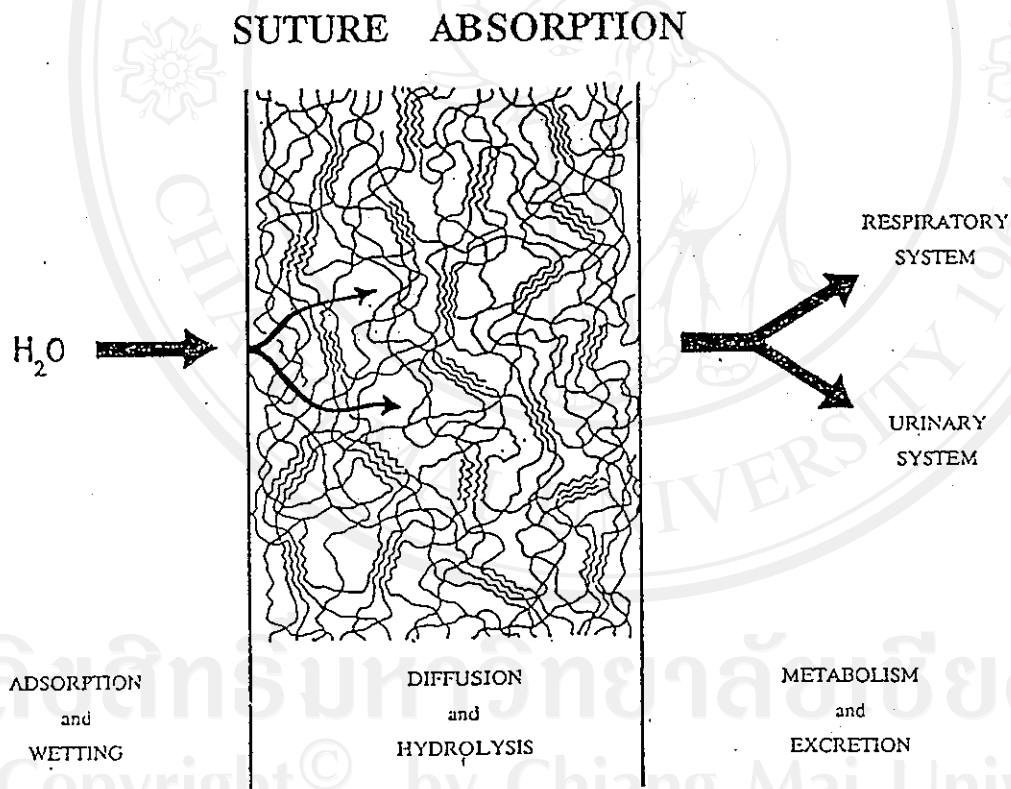


Fig. 5.6: The various processes involved in suture absorption.

Undoubtedly, the first step in any suture absorption is adsorption of water molecules and wetting at the polymer surface. The efficiencies and, therefore, the rates of these physical processes depend primarily on the hydrophilicity of the polymer.

This is then followed by hydrolysis at the surface leading to the formation of micro-defects which facilitate the diffusion of water into the bulk interior of the polymer matrix. The exact nature of these surface defects (i.e., whether they are pores or cracks, etc.) has apparently not been studied. As water diffuses into the polymer's semi-crystalline matrix, as shown in Fig. 5.6, hydrolysis occurs preferentially in the amorphous regions where the chains are more loosely packed than in the highly ordered-crystalline regions. While hydrolysis proceeds, the polymer molecular weight decreases until the degradation products are small enough in size to diffuse out of the matrix. As this becomes possible, the weight starts to decrease and the matrix becomes more porous, thus facilitating further diffusion in and out of water and products respectively. Eventually, as bulk erosion reaches an advanced stage, the suture fibres break up into small fragments, as indicated previously on Figs. 5.3 and 5.4.

Finally, in actual surgical use, the degradation products would eventually be removed from the suture site by the body's natural processes of metabolism and excretion. In the case of 'PDS II', the final products following metabolism are reported to be carbon dioxide and water [5]. The carbon dioxide is excreted in expired air while the water is excreted both in expired air and in the urine.

5.4 Comparison of Monofilaments

The 'in vitro' changes in mass, knot pull force, and intrinsic viscosity for 'Maxon' and 'PDS II' are compared in Figs. 5.7, 5.8 and 5.9 respectively, together with the data obtained for the two non-absorbables 'Prolene' and 'Ethilon'. Also included in Figs. 5.7, 5.8 and 5.9 are the corresponding profiles for 'PDS' obtained under identical experimental conditions in a similar study [27] carried out concurrently with this one.

MONOFILAMENTS

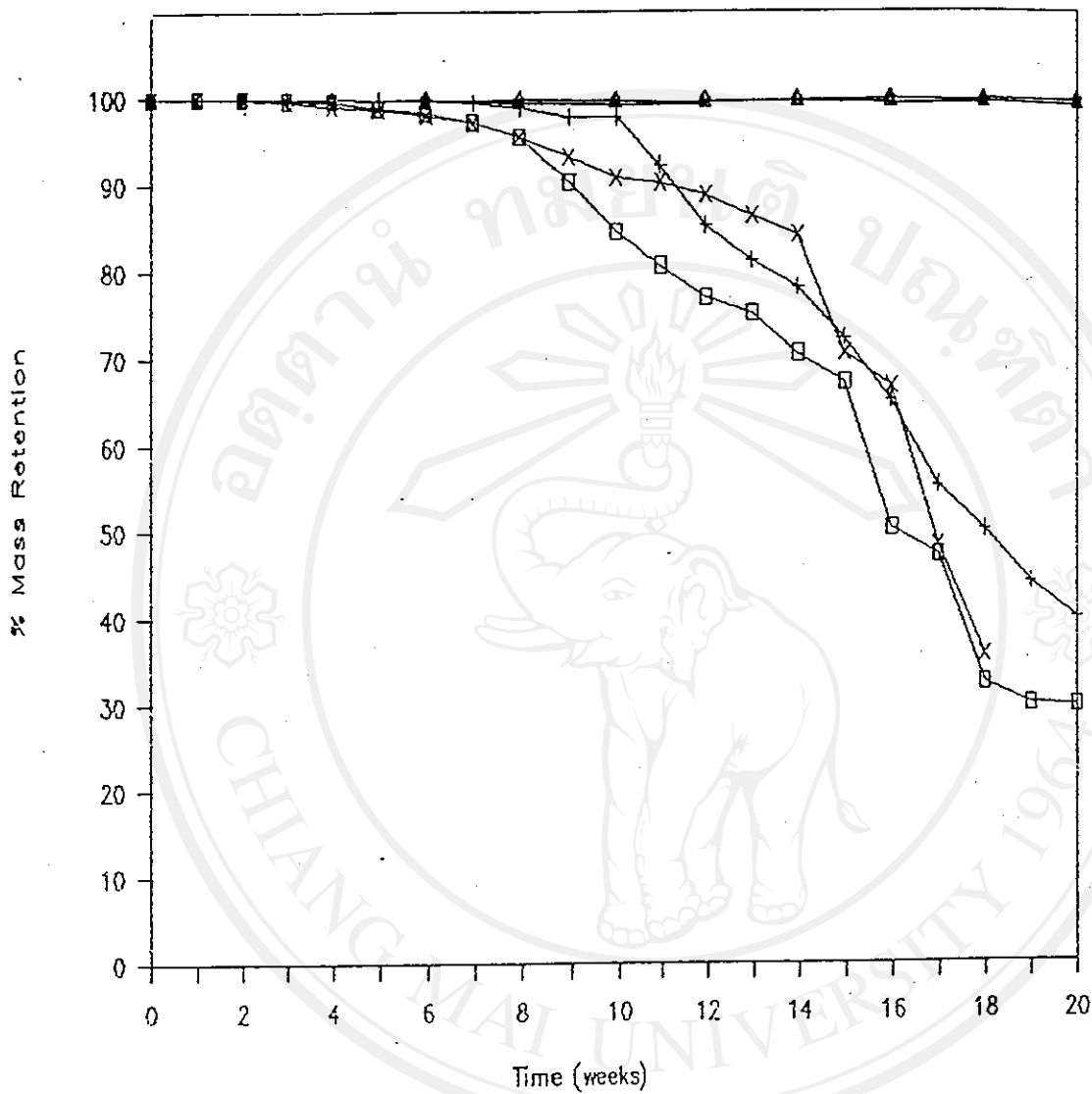


Fig. 5.7: Comparison of 'in vitro' % mass retentions of monofilament sutures in phosphate buffer (pH = 7.40) at 37°C.

Absorbable Sutures		Non-absorbable Sutures	
□	Maxon	▲	Prolene
×	PDS I	◇	Ethilon
+	PDS II	} superimposed	

MONOFILAMENTS

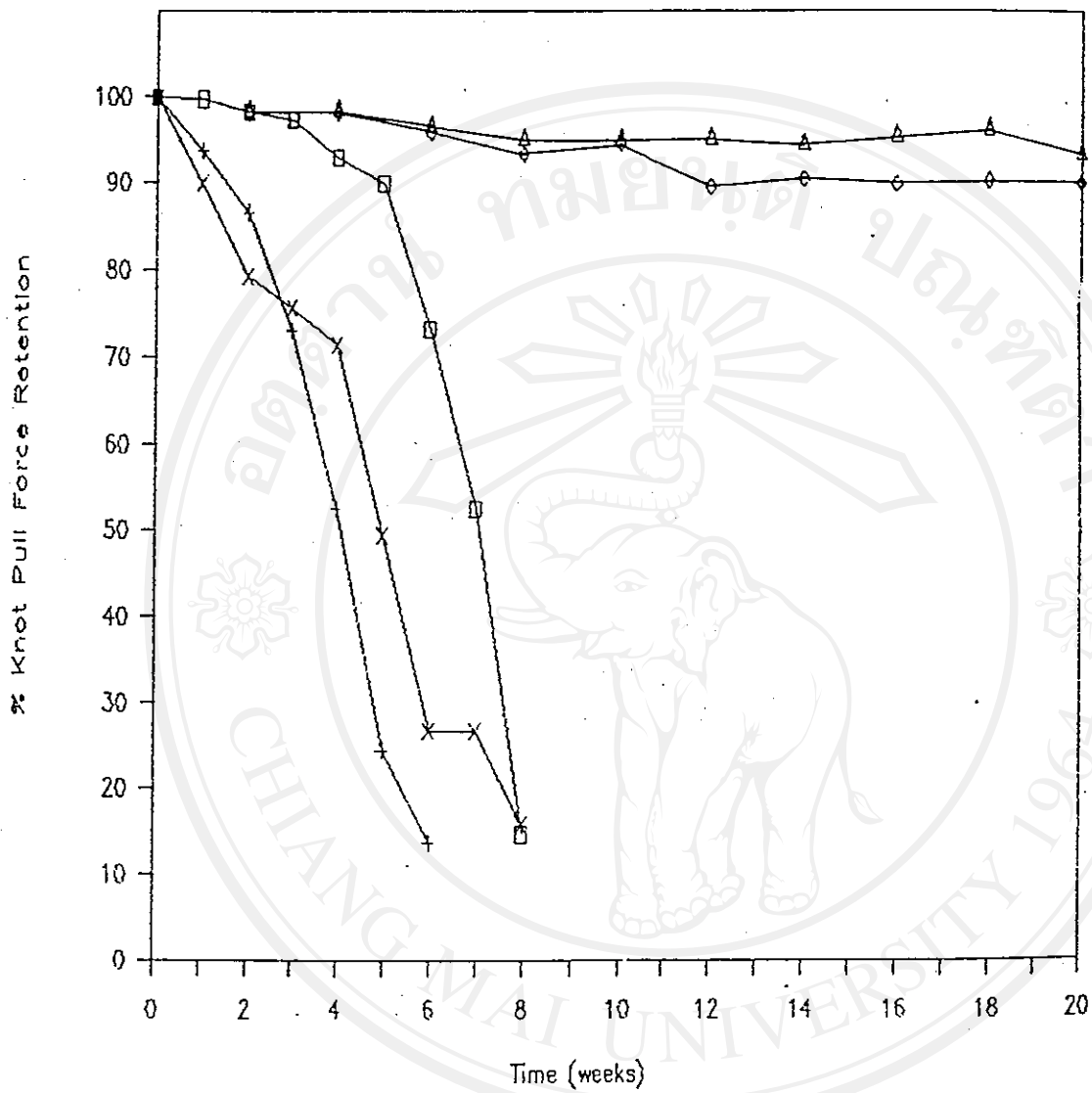


Fig. 5.8: Comparison of 'in vitro' % knot pull force retentions of monofilament sutures in phosphate buffer (pH = 7.40) at 37°C.

<u>Absorbable Sutures</u>		<u>Non-absorbable Sutures</u>	
□	Maxon	△	Prolene
×	PDS [27]	◇	Ethilon
+	PDS II		

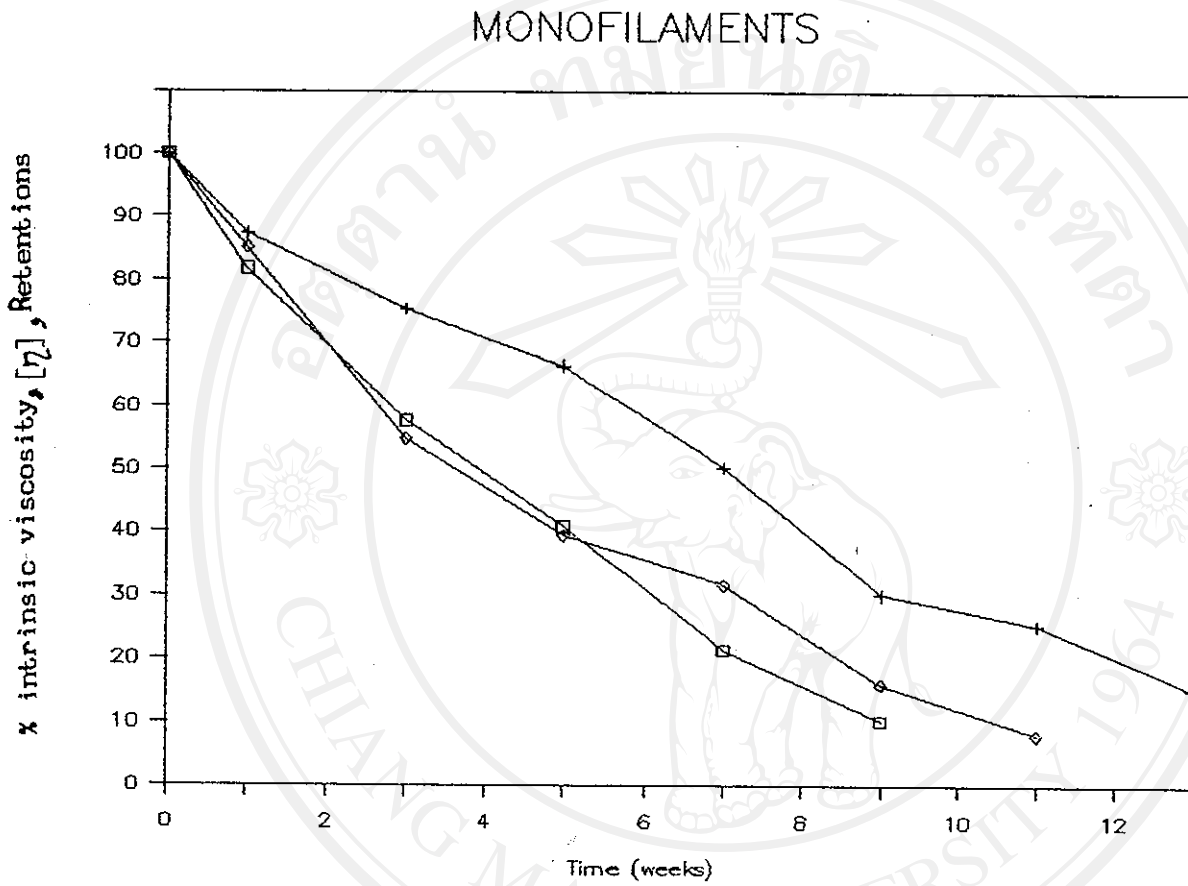


Fig. 5.9 : Comparison of 'in vitro' % intrinsic viscosity retentions of monofilament sutures in phosphate buffer (pH = 7.40) at 37°C.

- + Maxon
- PDS II
- ◇ PDS

ลิขสิทธิ์มหาวิทยาลัยเชียงใหม่
Copyright © by Chiang Mai University
All rights reserved

From Fig. 5.7, it can be seen that 'Maxon' (week 9) starts to lose weight before 'PDS II' (week 11), although their subsequent rates of weight loss are quite similar at about 5 - 6 % per week. 'PDS' seems to show an absorption profile intermediate between 'Maxon' and 'PDS II'. The two non-absorbable sutures, 'Prolene' and 'Ethilon', show negligible weight losses as expected.

However, this weight-related "order of stability" in Fig. 5.7 ('Maxon' < 'PDS II') is reversed in Fig. 5.8. In Fig. 5.8, the knot pull breaking force of 'PDS II' clearly decreases faster than 'Maxon'. 'PDS' is very similar to 'PDS II'. These knot pull force comparisons are supported by the intrinsic viscosity (molecular weight) trends in Fig. 5.9. Therefore, in terms of molecular weight reduction (i.e., hydrolysability), the "order of stability" changes to 'PDS II' < 'Maxon'.

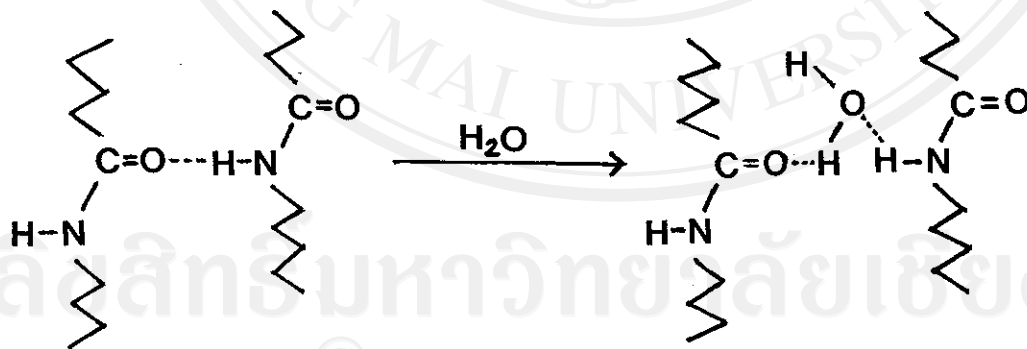
Since all of the monofilament sutures used in this work were of the same size (2-0), and therefore the same surface area-to-bulk ratio, the differences in their property-loss profiles can be attributed solely to the differences in their chemical structures.

$\left[\text{O-CH}_2\text{-CO} \text{-----} \text{O-(CH}_2\text{)}_3\text{-O-CO} \right]_n$	$\left[\text{O-CH}_2\text{CH}_2\text{-O-CH}_2\text{-CO} \right]_n$
<p>'Maxon'</p> <p>poly(glycolic acid-co-trimethylene carbonate)</p> <p>P(GA-co-TMC)</p> <p>GA : TMC = 67.5 : 32.5 (by mole)</p>	<p>'PDS II'</p> <p>poly-p-dioxanone</p> <p>(also 'PDS')</p> <p>difference undisclosed</p>

Thus, 'PDS II' is seemingly more hydrolysable than 'Maxon', presumably due to 'Maxon's' relatively hydrophobic trimethylene units, $\text{-(CH}_2\text{)}_3\text{-}$. However, it is these same trimethylene units which are also responsible for 'Maxon's' enhanced flexibility as a monofilament. Interestingly though, 'PDS II's' more rapid molecular weight decrease, complete within 9 weeks, does not lead to a more rapid weight loss. Instead, 'Maxon' starts to lose weight before 'PDS II'. What this means, in effect, is that, although 'PDS II' (and 'PDS') undergoes a more rapid molecular weight decrease, the hydrolysis fragments formed are less able to diffuse out of the degrading matrix than those in 'Maxon'. This illustrates the complexity of the ways in which the various physico-chemical processes influence each other in the overall absorption process. Chemical processes, such as hydrolysis, and physical processes, such as diffusion, each with their own rate constant, will be affected in different ways by factors such as hydrophilicity and matrix morphology (% crystallinity, crystalline packing), all of which relate back to the polymer's chemical structure.

To quantify all of these processes kinetically, especially in view of their interdependencies, would be an impossible task. Hence, we must satisfy ourselves with making the most of the qualitative comparisons which the combined data in Figs. 5.7 - 5.9 allows.

As a final comment on these monofilaments, it is interesting to note in Fig. 5.8 that 'Ethilon', one of the two non-absorbables, does show a slight decrease in knot pull breaking force with time. This is believed to be due to a 'plasticizing' effect of water molecules in 'nylons' (polyamides). This is caused by water molecules diffusing into the polyamide matrix and partially disrupting the intermolecular hydrogen bonding, as shown below. This forces the chains further apart, reduces the forces of attraction, and decreases the mechanical strength.



5.5 Comparison of Monofilaments and Multifilaments

The 'in vitro' performances of the three absorbable monofilaments - 'Maxon', 'PDS II' and 'PDS' [27] - are compared with those of the two absorbable multifilaments - 'Dexon' [28] and 'Vicryl' [29] - in Figs. 5.10, 5.11 and 5.12.

From Fig. 5.10, the marked difference in the absorption rates between the monofilaments and the multifilaments is clearly seen. The multifilaments lose weight much more quickly due to a combination of both physical and chemical factors:

- (1) the physical effect of a much higher surface area : bulk ratio; and
- (2) the chemical effects of greater hydrophilicity and hydrolysability.

This marked difference in terms of weight loss is much less pronounced in terms of both knot pull breaking force (Fig. 5.11) and intrinsic viscosity (Fig. 5.12). These latter properties are related almost exclusively to molecular weight changes and, therefore, hydrolysability. This, in turn, suggests that it is the physical effect of a much increased surface area : bulk ratio which is the more influential factor in increasing the overall rate of absorption. Increasing this ratio effectively increases the rates of diffusion of molecules in and out of the suture matrix, as visualized in Fig. 5.6 on page 101 previously. The increase in the rate of diffusion of

relatively large hydrolysis fragments out of the matrix is likely to be much more than the increase in the rate of small water molecules into the matrix.

Thus, the absorption profiles in Fig. 5.10 illustrate vividly the problems confronting polymer scientists in their quest for new, more flexible monofilaments. The current monofilaments, 'PDS II' and 'Maxon', are still considered by many surgeons to be too "springy" with poor knot security. To a certain extent, this is an inevitable consequence of their physical form as monofilaments. Also, the introduction of flexible bonds, such as $\text{-(CH}_2\text{)}_3\text{-}$ in 'Maxon' and -C-O-C- in 'PDS II', into their chemical structures to improve their handling characteristics automatically reduces hydrolysability and lengthens the absorption period. Absorption periods in excess of 6 months, as indicated for both 'PDS II' and 'Maxon' in Fig. 5.10, can lead to undesirable side effects in patients. An example is the formation of kidney stones within which cross-sections have revealed the presence of suture fragments. A satisfactory balance has yet to be reached between the handling and the healing characteristics in absorbable monofilaments.

MONOFILAMENTS versus MULTIFILAMENTS

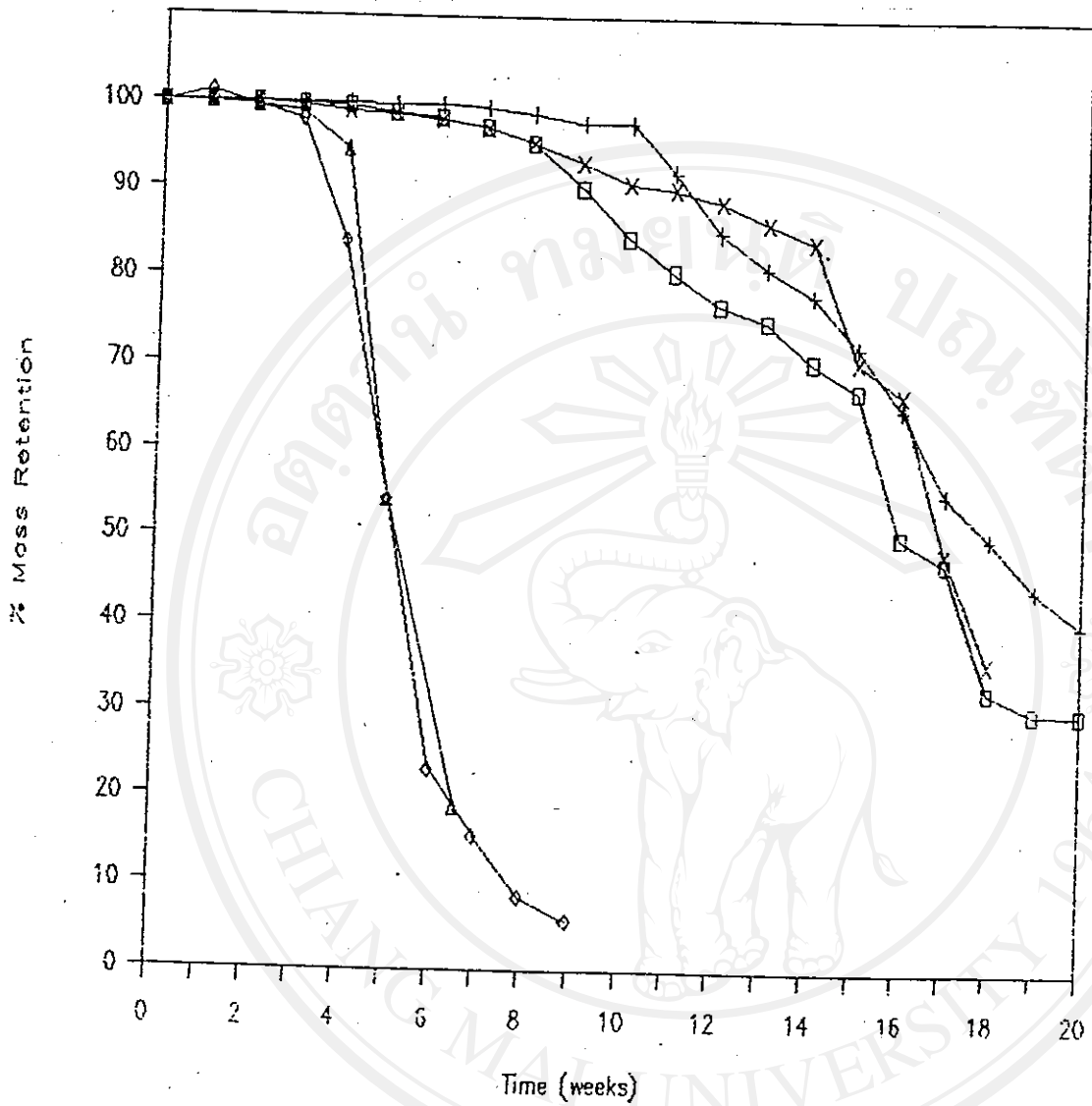


Fig. 5.10: Comparison of absorbable monofilament and multifilament sutures in terms of their % mass retentions (rates of absorption) in phosphate buffer (pH = 7.40) at 37°C.

MONOFILAMENTS

- Maxon
- × PDS [27]
- + PDS II

MULTIFILAMENTS

- △ Dexon [28]
- ◇ Vicryl [29]

MONOFILAMENTS versus MULTIFILAMENTS

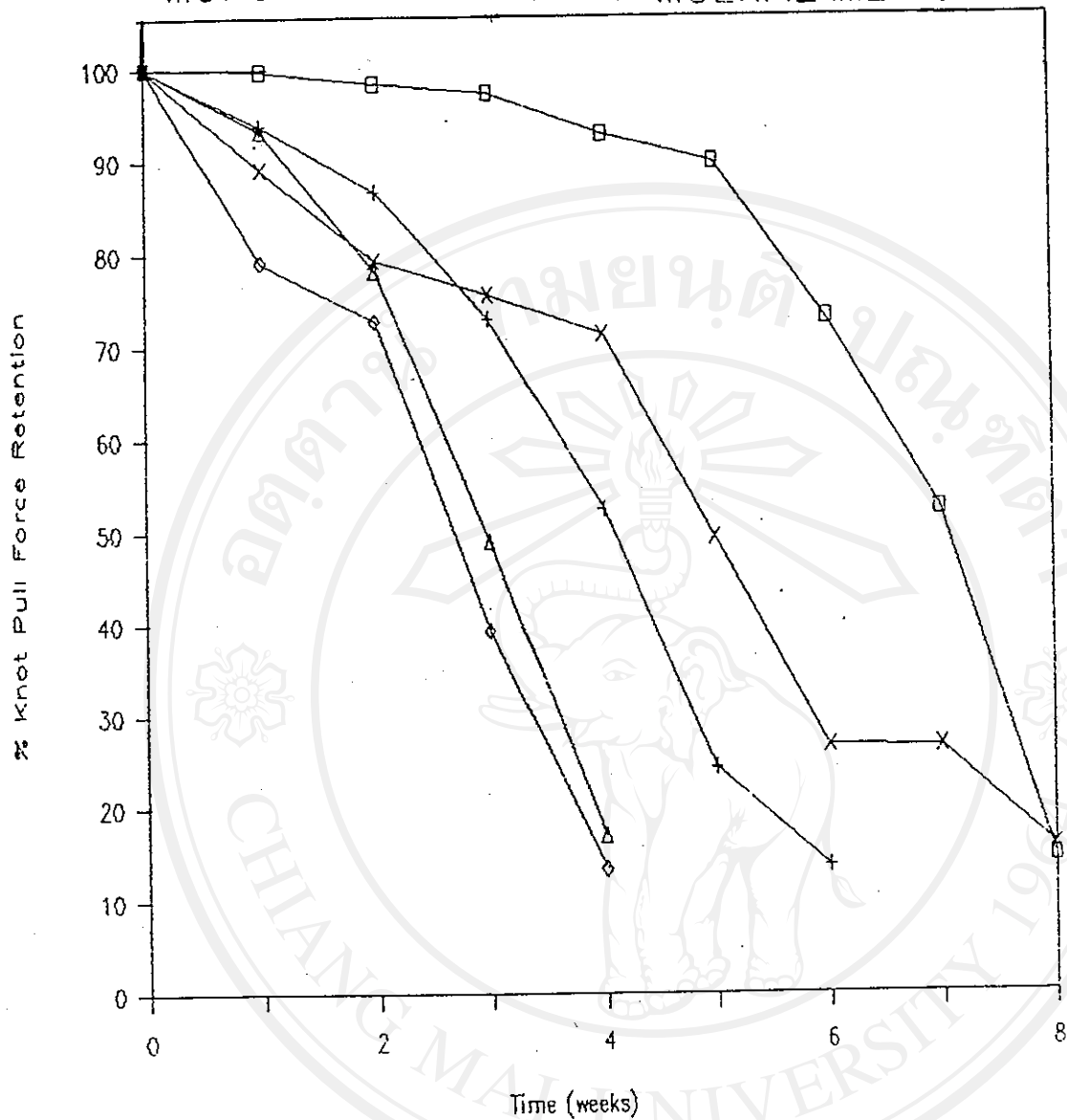


Fig. 5.11: Comparison of absorbable monofilament and multifilament sutures in terms of their % knot pull force retentions in phosphate buffer (pH = 7.40) at 37°C.

MONOFILAMENTS		MULTIFILAMENTS	
□	Maxon	△	Dexon [28]
×	PDS [27]	◇	Vicryl [29]
+	PDS 11		

MONOFILAMENTS versus MULTIFILAMENTS

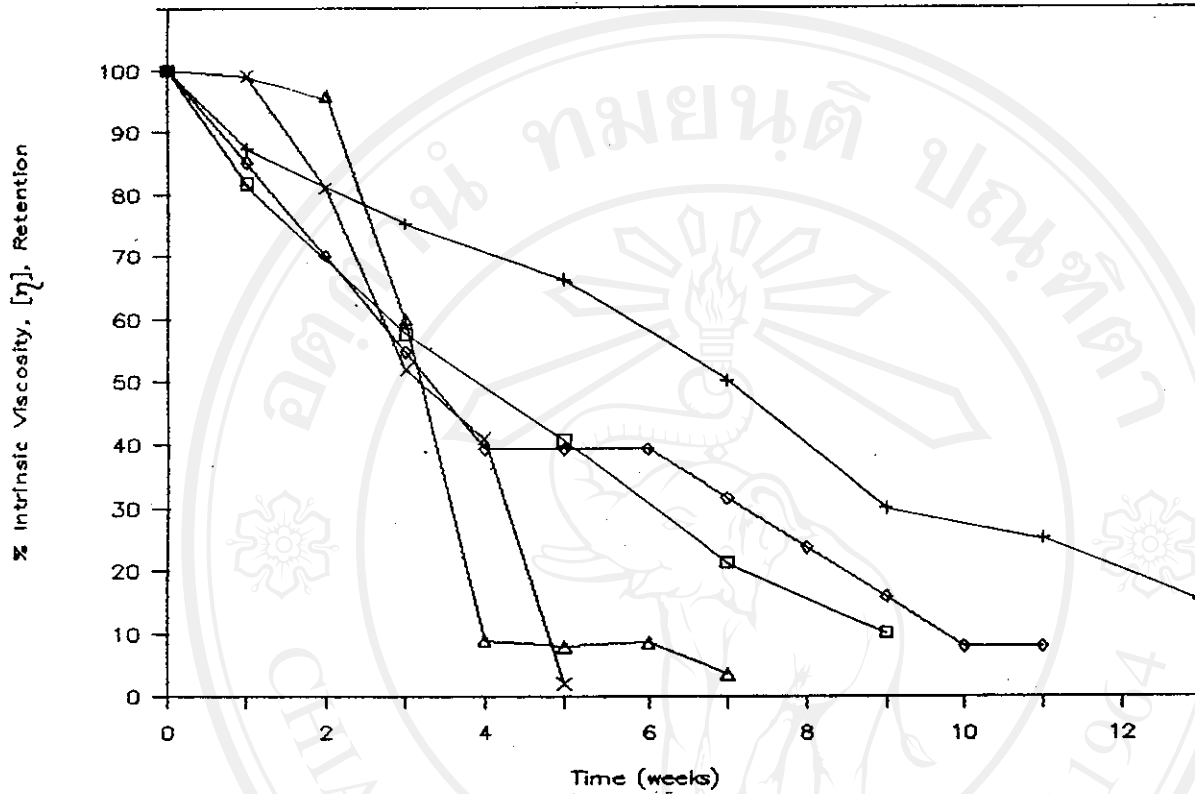


Fig. 5.12: Comparison of absorbable monofilament and multifilament sutures in terms of their % intrinsic viscosity retentions in phosphate buffer (pH = 7.40) at 37°C.

MONOFILAMENTS

+ Maxon

◇ PDS [27]

□ PDS II

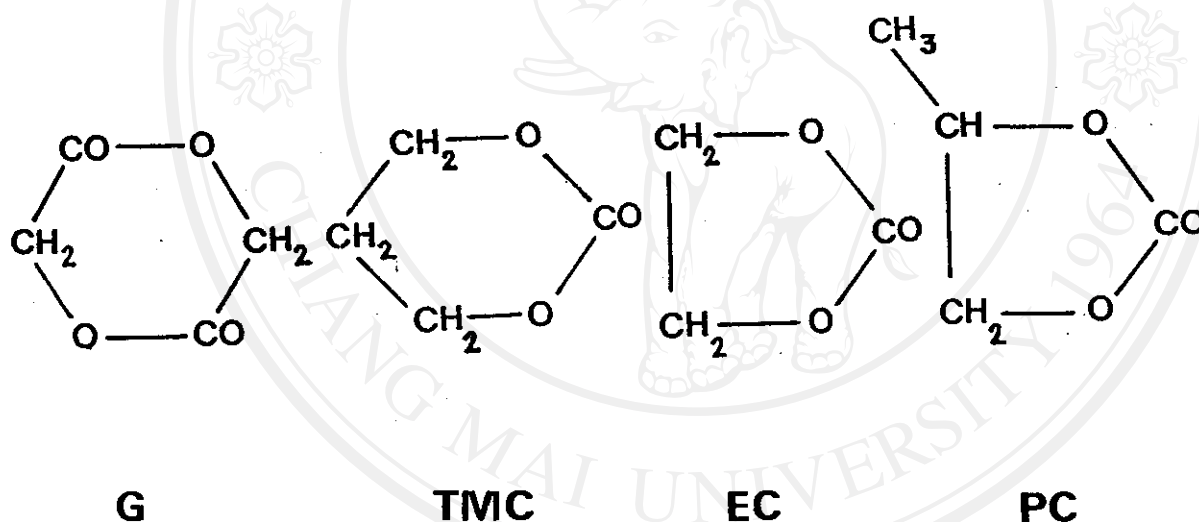
MULTIFILAMENTS

Δ Dexon [28]

X Vicryl [29]

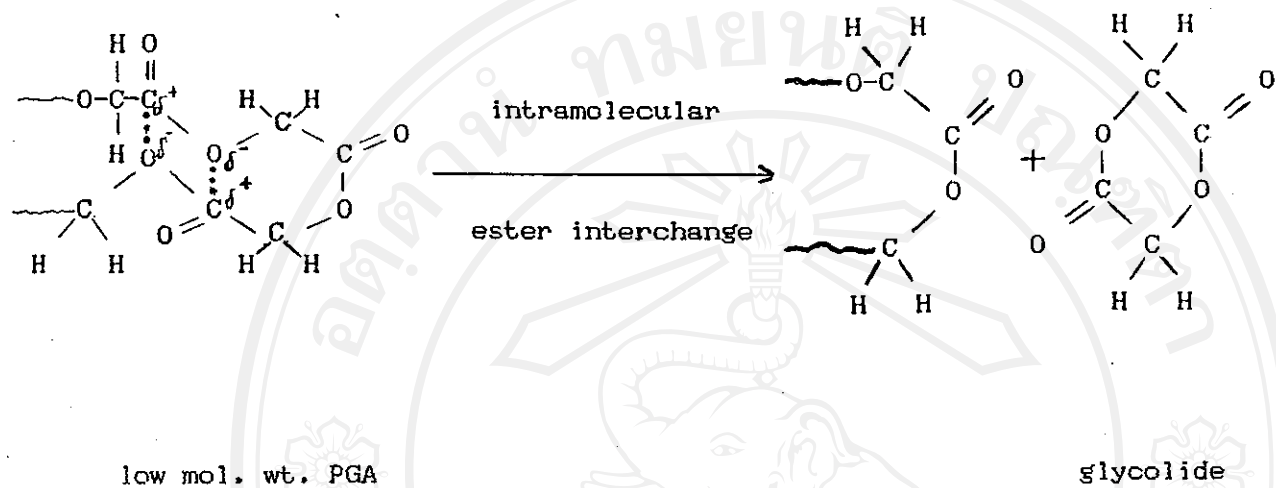
5.6 Copolymer Synthesis

In this final part of this research project, some preliminary studies were carried out into the synthesis of random copolyesters of chemical structures comparable to that of 'Maxon'. Two variations on the 'Maxon' structure were examined in which the trimethylene carbonate (TMC) modifying comonomer in 'Maxon' was changed to ethylene carbonate (EC) and propylene carbonate (PC). The main comonomer, glycolide (G), was retained.



Unlike ethylene carbonate and propylene carbonate which are readily available commercially, glycolide has to be itself synthesized from glycolic acid. It is generally accepted that glycolide is not formed directly from glycolic acid, but indirectly via the thermal decomposition of intermediate low molecular weight poly(glycolic acid) (PGA) oligomers. This thermal decomposition occurs via an intramolecular ester interchange mechanism, as also proposed for other members of the poly- α -ester series[30-32]. This mechanism is shown in

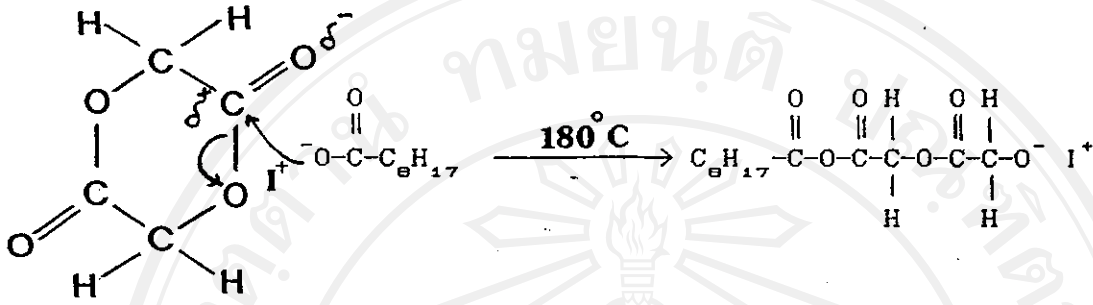
Scheme 5.1. Antimony trioxide was used as a catalyst in this thermal decomposition step.



Scheme 5.1: Mechanism of thermal decomposition of low molecular weight poly(glycolic acid) to glycolide.

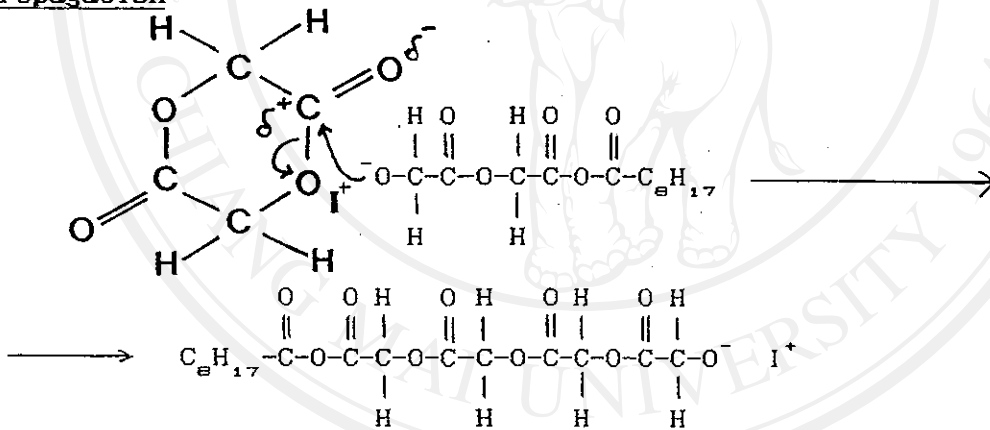
In these copolymer syntheses, stannous octoate, $\text{Sn}(\text{C}_8\text{H}_{17}\text{COO})_2$ was used as the initiator. Stannous octoate is generally considered to be an anionic-type initiator, acting via the mechanism shown in Scheme 5.2 for the ring-opening polymerisation of glycolide. Similar mechanisms can be drawn for the ring-opening of ethylene carbonate and propylene carbonate. In each case, nucleophilic attack of the initiating octoate anion occurs at the carbonyl-carbon of the monomer ring. The ring then opens in such a way as to form the more stable propagating anion.

1. Initiation



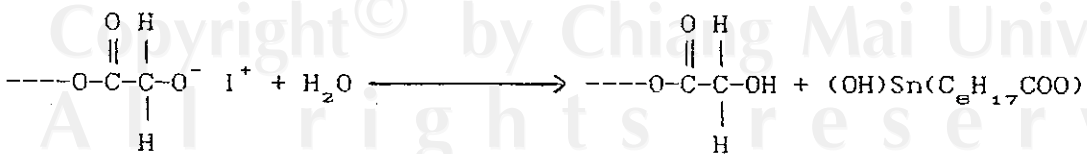
where $\text{I}^+ = [\text{Sn}(\text{C}_8\text{H}_{17}\text{COO})]_2^+$ counterion

2. Propagation



3. Termination

E.g., by chain transfer to adventitious moisture impurities



Scheme 5.2 : Anionic ring-opening polymerisation of glycolide using stannous octoate as initiator.

In the case of copolymerisation, the composition of the copolymer formed depends primarily on the comonomer feed and the respective comonomer reactivity ratios. While the comonomer feed can be controlled, the comonomer reactivity ratios cannot. In the systems studied here, these ratios are a measure of the relative polymerisabilities of the two comonomers towards the respective anions. The polymerisability of a ring compound depends on various factors such as:

- (1) the nature of the atoms in the ring;
- (2) ring-size and the extent of ring-strain;
- (3) the nature of any substituents on the ring;
- (4) the type of initiator used;
- (5) the experimental conditions employed for the copolymerisation reaction.

Since the relative reactivities of the three cyclic monomers studied here (G, EC and PC) were unknown, equimolar comonomer feeds were employed in the two G/EC and G/PC copolymerisations. The melting ranges of the final P(G-co-EC) and P(G-co-PC) copolymers are compared in Table 5.1 alongside those of PGA homopolymer, 'Maxon' and 'PDS II'. Their IR spectra and dynamic TG thermograms were compared earlier in Chapter 4 in Figs. 4.6/page 86 and Fig. 4.7/page 90 respectively.

Table 5.1: Comparison of melting ranges of commercial monofilaments and the final products synthesized in this work.

Commercial and Synthesized Products	Melting Range (°C)
'Maxon'	192-215
'PDS II'	93-112
PGA	190-200
P(GA-co-EC)	200-210
P(GA-co-PC)	195-215

From the results in Table 5.1, it would seem from their high melting ranges that the synthesized products are all relatively high molecular weight materials. However, it is still unclear as to whether the two copolymers, P(G-co-EC) and P(G-co-PC), are true homogeneous random copolymers or are mixtures containing homopolymer fractions, as represented by:

PG / P(G-co-EC) / PEC

and PG / P(G-co-PC) / PPC

Furthermore, if they are mixtures, they may be completely compatible, partially compatible, or incompatible blends. In order to resolve these uncertainties, much more detailed structural and compositional analyses than those possible in this study need to be carried out. This should form the central theme of a future research project in this important area of product development.

Other suggestions for further work are now also made in conclusion of this thesis.



ลิขสิทธิ์มหาวิทยาลัยเชียงใหม่
Copyright© by Chiang Mai University
All rights reserved